第 28 卷第 3 期 无 机 化 学 学 报 Vol.28 No.3
2012 年 3 月 CHINESE JOURNAL OF INORGANIC CHEMISTRY 584-590

一种复合熔融碳酸盐燃料电池基体阴极的制备和性质研究

陈丽江* 刘海华 董晓玲 洪小平 贾彦荣 徐火英
(浙江理工大学理学院化学系,杭州 310018)

摘要: 采用电泳沉积技术将 $LiCoO_2$ 和 CeO_2 两种纳米颗粒同时沉积至多孔镍基阴极表面, 获得一种新型复合基体阴极材料——$LiCoO_2$-CeO_2-Ni。研究了其在模拟熔融碳酸盐燃料电池(MCFC)工作条件下的形变/溶解行为,并对其实验前后的表面进行了详细分析。结果表明,与传统多孔镍基阴极相比,新基体阴极材料在模拟 MCFC 启动及运行条件下形变微小,镍溶出速率低。材料表面所修饰的纳米颗粒薄层对镍基体包覆致密且与之形成稳定新相,从而有效抑制了材料的形变和溶解。

关键词: 燃料电池; 复合基体阴极; 纳米颗粒; 形变/溶解; 表面分析
中图分类号: O614.81+3; TM911.4; TB333 **文献标识码**: A **文章编号**: 1001-4861(2012)03-0584-07

Preparation and Property of a Composite-Based Cathode for Molten Carbonate Fuel Cells

CHEN Li-Jiang* LIU Hai-Hua DONG Xiao-Ling HONG Xiao-Ping JIA Yan-Rong XU Huo-Ying
(*Department of Chemistry, Zhejiang Sci-Tech University, Hangzhou* 310018, *China*)

Abstract: A composite-based cathode ($LiCoO_2$-CeO_2-Ni) for molten carbonate fuel cells (MCFCs) was prepared by electrophoretic deposition (EPD) technique using two kinds of nanoparticles, $LiCoO_2$ and CeO_2. The deformation and dissolution of the base cathode were studied under simulated conditions of MCFC and the cathode surface was also analyzed. The results indicate that the base cathode has a negligible deformation and a lower dissolution rate compared with that of the Ni-based cathode. The nanoparticles layer on the surface of the cathode is very compact and the nanoparticles combine well with Ni matrix to form a stable new phase, which can effectively inhibit the deformation and dissolution of the material.

Key words: fuel cells; composite-based cathode; nanoparticles; deformation/dissolution; surface analysis

The molten carbonate fuel cell (MCFC) is expected to be one of the most promising energy conversion devices that convert chemical energy directly into electricity. It is also a highly efficient and environmentally clean source of power. However, the degradation of cathode materials due to NiO dissolution problem is one of the major lifetime-limiting factors of the molten carbonate fuel cell[1]. Considerable efforts have been devoted to solve this problem, such as using alternative electrolyte or adding alkaline earth metal salts into electrolyte[1-2], developing alternative cathode materials[3] etc.. Among them, $LiFeO_2$ cathode shows a negligible dissolution rate but unfortunately a very low performance probably due to the properties of intrinsic materials, such as poor catalytic activity and electrical conductivity[3-4]. $LiCoO_2$ was considered the most promising alternative cathode material due to its low solubility in molten carbonate and acceptable electrochemical performance compared with NiO[3-7]. So far, no candidate material made of a single component can

收稿日期:2011-07-21。收修改稿日期:2011-12-16。
国家自然科学基金(No.20803067),浙江省钱江人才计划(No.2009R10029)和浙江省自然科学基金(No.Y4100191)资助项目。
*通讯联系人。E-mail:chenlj@zstu.edu.cn,Tel:+86-571-86843781;会员登记号:S060017470M。

totally substitute lithiated NiO. Advantages of NiO in aspect of electric conductivity and electrochemistry are very attractive and are desired to be preserved in new materials, and thus new cathode materials containing NiO composition are promising for MCFC and have been investigated to some extent[8-12]. Surface modification of the electrode material is considered as an effective method for improving the surface properties while maintaining bulk properties of the material. Many attempts have been made to cover NiO surface with some layers of stable materials so as to alleviate NiO dissolution[7,14-27]. The stable materials coated on NiO/Ni surface mainly encompass $LiCoO_2$[7,14-16], CoO[17-18], Co_3O_4[19-21], CeO_2[23-24], $LiFeO_2$[25], Co[26-27]. Hereinto, oxides of cobalt are the most commonly used coating materials because they are capable of forming a stable new phase on the surface of nickel matrix by interacting with nickel in electrolyte. In addition, materials made of /or modified by some of rare earth oxides are also thought as promising cathodes for MCFC[4,11-13]. And the cathode of NiO coated with Ce implies a greater endurance and possesses a better cell performance than that of the commercial nickel cathode[23].

In this work, the intention is to modify Ni-based cathode with a mixture of $LiCoO_2$ and CeO_2 nanoparticles by use of electrophoretic deposition (EPD) technique so as to obtain a new base-cathode, $LiCoO_2$-CeO_2-Ni. The surface of the new material was characterized. Compared with those of Ni-based cathode, the deformation and dissolution of the new material are remarkably reduced under conditions of a simulated startup stage of a MCFC. The new base cathode with good mechanical strength is convenient for installation of MCFC stack, and is able to convert in situ into $LiCoO_2$-CeO_2-NiO working cathode, which is expected to have good performances and to be useful for application in MCFC.

1 Experimental

1.1 Synthesis and characterization of nanoparticles

The two nanoparticles, $LiCoO_2$ and CeO_2, were synthesized by using metal nitrates, such as $LiNO_3$, $Co(NO_3)_2\cdot 6H_2O$ and $Ce(NO_3)_3\cdot 6H_2O$ (purity: 99%; Shanghai Hengxin Chemical Reagent Co. Ltd., China), as the starting materials and citrate acid as the fuel of gel combustion. In the preparation for $LiCoO_2$ particles, stoichiometric amounts of $LiNO_3$, $Co(NO_3)_2\cdot 6H_2O$ and citric acid were thoroughly mixed in distilled water by using a hot plate with magnetic stirrer, at 95 ℃ for about 2 h to obtain a viscous resin. Thereafter the viscous resin was dried up in an oven at 135 ℃, and subsequently charred to ash at 350 ℃, and then calcined at 650 ℃ for 2 h in air. Similar to the preparation for $LiCoO_2$, stoichiometric amounts of $Ce(NO_3)_3\cdot 6H_2O$ and citric acid were thoroughly mixed, and then the same procedure was followed to obtain CeO_2 particles. The phase analysis for the two nanoparticles was carried out with X-ray diffractormeter (XRD, D8 Discover, Germany) under the following conditions: graphite monochromatic copper radiation (Cu $K\alpha$, λ =0.154 18 nm); sodium iodide scintillation detector; 40 kV as accelerating voltage; 40 mA as emission current; and the 2θ range of 10° ~90° for $LiCoO_2$ and of 20°~120° for CeO_2 at a scan rate of 4°·min^{-1}. The size of $LiCoO_2$ and CeO_2 were estimated using the Scherrer equation. The morphology of the particles was characterized by Transmission Electron Microscopy (TEM, JEOL-2010, Japan) under conditions of 100 kV accelerating voltage and LaB_6 filament.

1.2 Preparation and characterization

Electrophoretic deposition was performed in suspension, consisting of the two nanoparticles and suitable dispersant, which was chosen on the basis of experiments conducted to measure the transparency of the suspension. In the dispersant (25 mL isopropanol), both particles (0.100 0 g, $LiCoO_2$ and CeO_2 with a molar ratio of 4:1) were well dispersed. The scheme for process of EPD was shown in Fig.1. The suspension was thoroughly mixed and adjusted to a fit pH value (2~5). Subsequently the nanoparticles of $LiCoO_2$ and CeO_2 with a molar ratio of 4:1 in the suspension were deposited simultaneously onto surface of porous nickel, which was used as the cathode, and platinum foil was used as the anode. In this process, the morphology and deposit thickness on the surface of the porous nickel

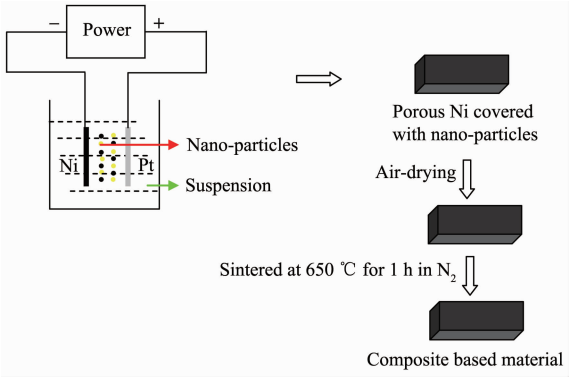

Fig.1 Scheme for preparation of composite-based cathode

can be mainly controlled by the parameters such as deposition voltage, time, pH value, and concentration of suspension, given the distance between the two electrodes is fixed. The samples were dried adequately and weighed accurately before and after the deposition in order to estimate a weight gain (Electronic analytical balance, FA2004, Shanghai, China). And the deposited samples were sintered at 650 ℃ in N_2 atmosphere for 1 h. Scanning electron microscopy (FE-SEM, ULTRA™ 55, Germany) with 15 kV accelerating voltage and 10 μA current and energy dispersive X-ray spectroscopy (EDX, Horiba EX-200, Germany) coupled with SEM were employed in the microstructural and componential analysis for the deposited samples.

1.3 Deformation/dissolution tests

The in situ deformation-measuring system and the experimental details have been described in reference[28]. Similar to the previous test, the deformation of a 1 cm^2 sample was tested in 3 g $(Li_{0.62}K_{0.38})_2CO_3$ at 650 ℃, and the experimental atmosphere was a mixture of CO_2, O_2 and N_2 gases with the volume ratio of 0.20:0.15:0.65 at a flow rate of 75 mL·min^{-1}. The load applied to the sample was about 3.51 ×10^5 N·m^{-2}. Following the deformation tests, surface carbonate was removed, and the post-experimental sample was then characterized by SEM. The corresponding solubility of nickel ions was determined by atomic absorption spectrophotometer (AAS, Sollar M6, USA), after the melt was dissolved with HNO_3 and brought to a constant volume of 250 mL using distilled water.

2 Results and discussion

Fig.2 shows the XRD patterns and TEM micrographs of $LiCoO_2$ and CeO_2 nanoparticles calcined at 650 ℃. According to the Scherrer equation: $D = 0.89\lambda/(B\cos\theta)$ (eq. **1**) (D is the crystallite size, λ the wavelength of the radiation, B the corrected peak width at half-maximum intensity, and θ the peak position), the crystallite size of $LiCoO_2$ was about 30.71 nm and that of CeO_2 was 16.43 nm. From the TEM images as shown in Fig.2, nanosized $LiCoO_2$ and CeO_2 grains could be clearly observed. The results indicate that both kinds of particles possess good crystallinity and relatively uniform size in nano scale.

Many EPD experiments were carried out in order to acquire ideal composite-based cathode possessing good morphology and thin depositing layer. Fig.3 indicates that the morphology and composition of the samples obtained under optimal preparation conditions. The covering layer, consisting of nanoparticles, was uniform and compact. The thickness of the layer was

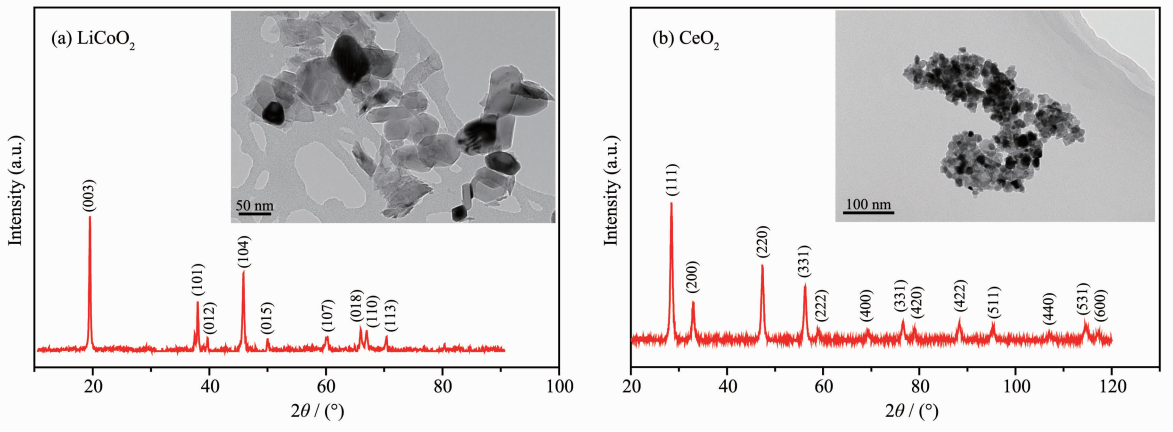

Fig.2 XRD patterns and TEM images of (a) $LiCoO_2$ and (b) CeO_2 nanoparticles prepared at 650 ℃

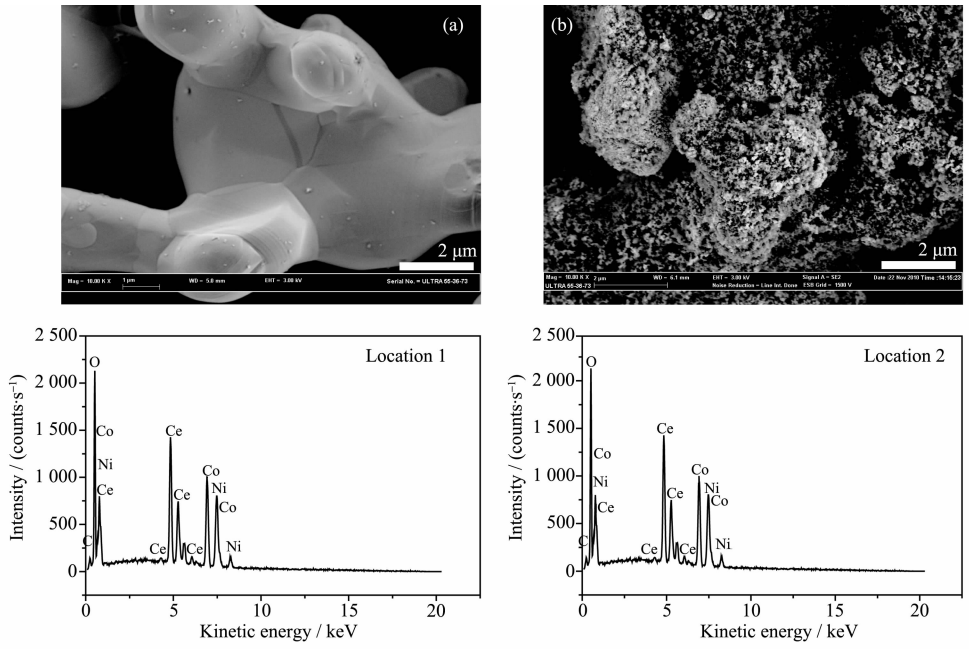

Fig.3　SEM images of porous (a) nickel and (b) $LiCoO_2$-CeO_2-Ni

thin enough to maintain the original porous structure as shown in Fig.3(a). The cobalt and cerium were observed in EDS spectra of the samples, proving that the two types of nanoparticles were simultaneously modified on the surface of porous nickel. However, it is noted that the molar ratio of Co/Ce in the coating is about 2 instead of 4 in the suspension. The result manifests that CeO_2 particles are more easily deposited than $LiCoO_2$, probably due to the smaller size of CeO_2 (~16 nm) than that of $LiCoO_2$ (~30 nm) in this work. The XRD results are shown in Fig.4. In the XRD pattern of porous nickel, the major peaks appear at 44.6°, 51.9°, 76.5°, 93.0°. Compared with that of porous nickel, two new weak peaks appear at 19.0° and 28.5° for the XRD pattern of the deposited sample shown in Fig.2, which are respectively designated as characteristic peak of $LiCoO_2$ and CeO_2. The low intensities for the new peaks are possibly attributed to a minor amount of nanoparticles, which forms the thin coating on the nickel surface and only produces about 1% weight gain. The XRD result also manifests that both nanoparticles, $LiCoO_2$ and CeO_2, are simultaneously modified on the surface of the porous nickel, in good agreement with EDS result mentioned above.

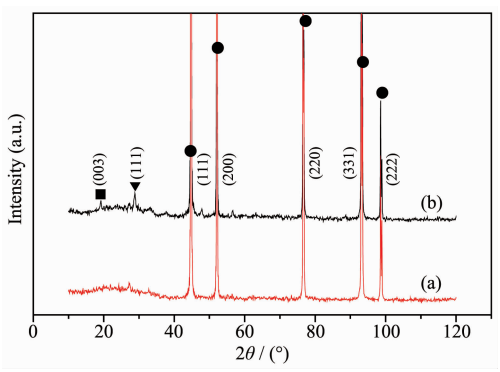

■: $LiCoO_2$, ▼: CeO_2, ●: Ni

Fig.4　XRD patterns of porous (a) nickel and (b) $LiCoO_2$-CeO_2-Ni

Early deformation of cathode material, occurring in the startup stage of actual MCFC, has also been confirmed to be a potential danger to short circuit and to be another significant factor resulting in short cell life[28]. Therefore, the deformation and dissolution of base cathode materials were studied under conditions of a simulated startup stage of a MCFC and the results are shown in Fig.5. Curve (a) indicates that the porous nickel deforms severely during its in situ oxidization/lithiation. Compared with the porous nickel, the composite-based cathode, $LiCoO_2$-CeO_2-Ni, has only minor deformation in the process of transforming in situ into the working cathode, as shown by Curve (b).

Fig.6 presents SEM images of post-test samples after removal of surface carbonates. Compared with that of the pretest porous nickel, the morphology of the post-

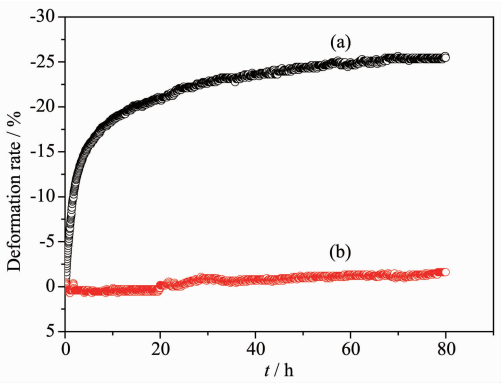

Fig.5 Deformation curves of porous (a) nickel and (b) $LiCoO_2$-CeO_2-Ni during their oxidation/lithiation in molten carbonate under a load of 3.51×10^5 N·m^{-2} in cathodic atmosphere

test nickel is obviously changed and lots of needle projections appear on the sample surface. The projections are presumed that the dissolving nickel ions in melts re-precipitate on the surface of materials by combining oxide ions[28]. On the contrary, no needle projections are observed on the surface of the composite material, instead, a uniform layer consisting of nanoparticles of $LiCoO_2$/CeO_2 is found to cover the surface as it is pre-tested. The results from EDS mapping images in Fig.7 for the post-experimental composite show that elements in the layer, Co and Ce, distribute homogeneously and are in accordance with Ni element in the matrix, manifesting that the deposited layer after tests is still uniform and compact. XRD peaks of NiO, instead of those of Ni, are found in the XRD pattern of the post-test composite sample in Fig.8 (c). The XRD peak for CeO_2 at 28.5° is still observed, while that for $LiCoO_2$ disappears. The XRD results manifest that the composite-based cathode, $LiCoO_2$-CeO_2-Ni, has transformed into $LiCoO_2$-CeO_2-NiO working cathode after tests. Moreover, by interacting with Ni and O during the oxidation/lithiation of the composite-based cathode, $LiCoO_2$ on the surface probably forms a new phase, resulting in the disappearance of $LiCoO_2$ peak at 19°. Existence of the new phase on the surface is confirmed by followed Raman analysis. As can be seen from Fig.9(a), the spectrum for $LiCoO_2$ powder has two strong Raman bands at 485 and 597 cm^{-1}. By contrast, the spectrum of the $LiCoO_2$-NiO (in Fig.9(b)) only has one broad band at 511 cm^{-1}, which is assigned to the new phase of $LiCo_yNi_{1-y}O$ that possesses a very slow dissolution rate and good electrochemical performance[14-15]. The Raman

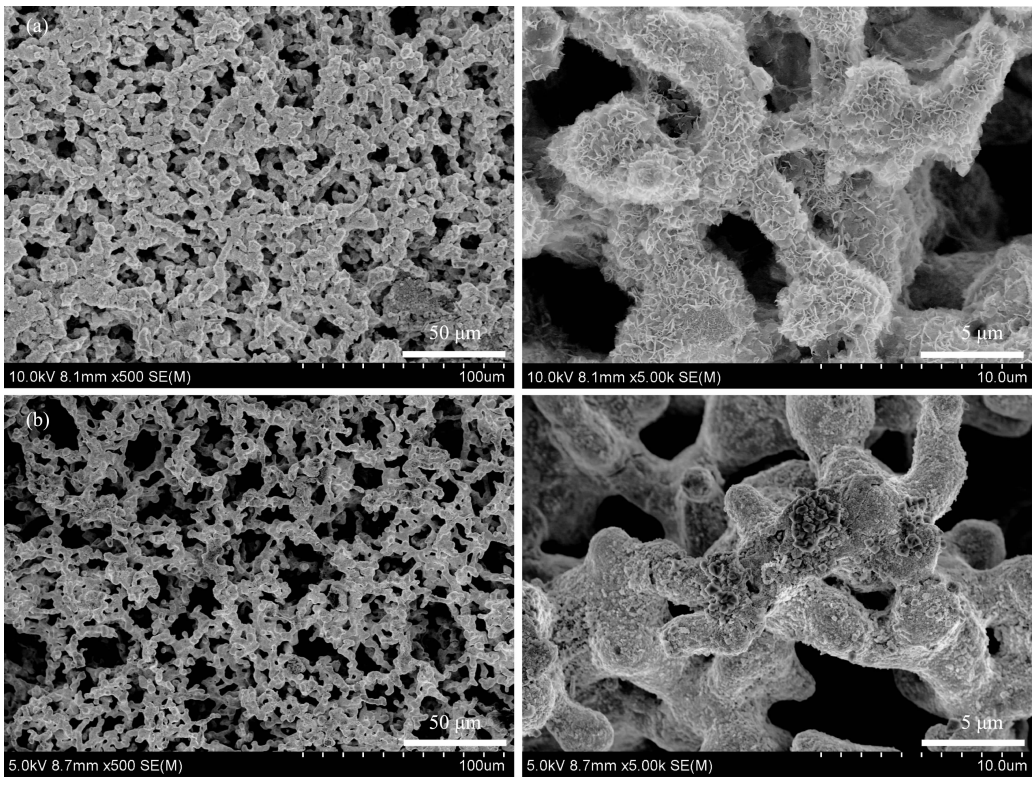

Fig.6 SEM images of post-experimental porous (a) nickel and (b) $LiCoO_2$-CeO_2-Ni

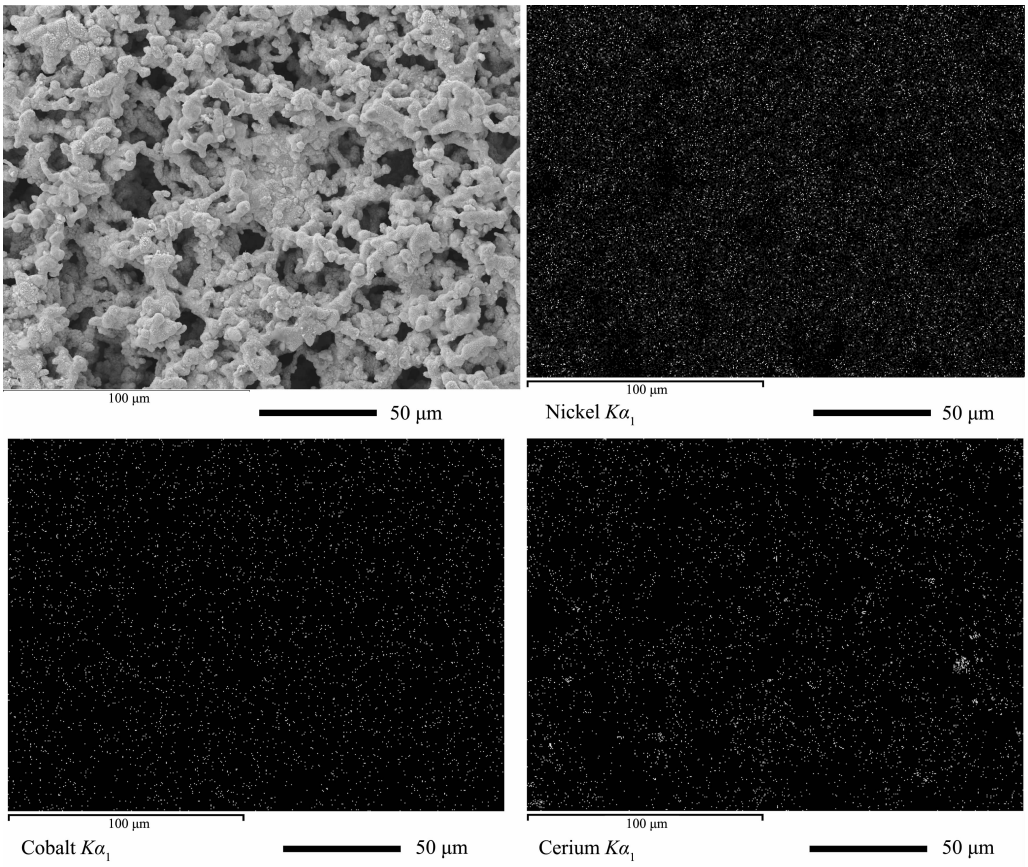

Fig.7　SEM image and nickel, cobalt and cerium elements mapping images of the post-test $LiCoO_2$-CeO_2-Ni

spectrum of the $LiCoO_2$-CeO_2-NiO cathode (Fig.9 (c)) shows not only a broad band at 511 cm^{-1} but also a weak band at 465 cm^{-1}, which is attributed to CeO_2 vibration. Therefore, Raman spectra in Fig.9 prove the formation of $LiCo_yNi_{1-y}O$ new phase and the presence of CeO_2 on the surface of the ternary composite material after tests.

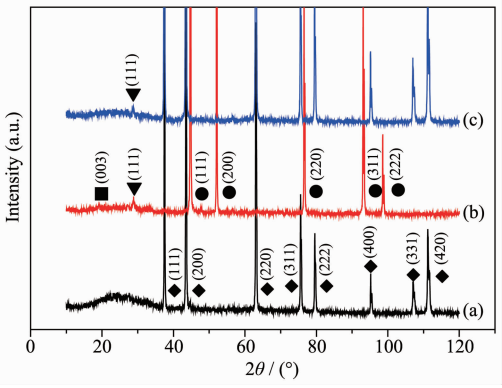

■: $LiCoO_2$, ▼: CeO_2, ●: Ni, ◆: NiO

Fig.8　XRD patterns of (a) NiO, (b) $LiCoO_2$-CeO_2-Ni before deformation test, (c) $LiCoO_2$-CeO_2-Ni\ after deformation/dissolution test of 80 h

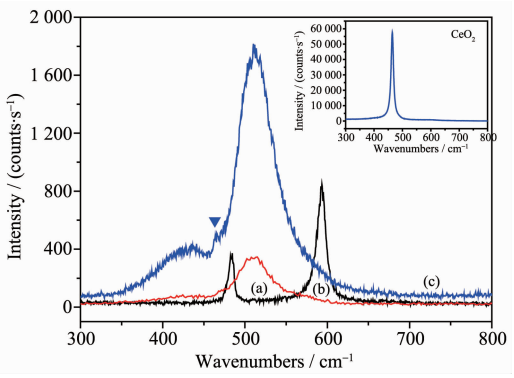

Fig.9　Raman spectra of (a) $LiCoO_2$ powder, (b) $LiCoO_2$-Ni after test, (c) $LiCoO_2$-CeO_2-Ni after test

Table 1 shows the concentration of nickel ions in Li/K_2CO_3 melts after deformation tests. The nickel solubility of $LiCoO_2$-CeO_2-Ni sample is greatly reduced

Table 1　Concentration of nickel ions in $(Li_{0.62}/K_{0.38})_2CO_3$ after deformation tests for 80 h

After 80 h deformation test	$c_{Ni^{2+}}$ / (mg·L^{-1})
Porous Ni	2.893 6
Porous $LiCoO_2$-CeO_2-Ni	0.862 9

compared with that of pure porous nickel. The mechanism of deformation and dissolution of porous nickel during oxidatin/lithiation under a load has been elucidated[28-29]. The thin NiO layer on the surface of porous nickel is inclined to spall into the melts due to CO_2 gas evolution when the molten carbonate decomposes to supply the oxide ions consumed by the oxidation of nickel during the oxidation /lithiation, and the load applied to sample accelerates the spalling. Accordingly, it can be deduced that the compact ceramic layer modified on the surface of porous nickel can avoid a direct contact between porous nickel and molten carbonates, thus effectively precluding the earlier NiO layer from spalling into melts during oxidation/lithiation of nickel, moreover, the new highly lithiated phase formed on the surface of the composite-based cathode is quite stable in the melts and can thus further inhibit the nickel dissolution.

3 Conclusions

A base cathode material for molten carbonate fuel cells, $LiCoO_2$-CeO_2-Ni, was prepared by EPD technique. SEM, EDS and XRD results for the composite material indicate that the two kinds of nanoparticles, $LiCoO_2$ and CeO_2, are simultaneously modified on the surface of porous nickel and form a uniform and compact thin layer. The composite material possesses a very good anti-deformation performance and a low dissolution rate, due to the presence of compact ceramic layer on nickel surface. Therefore, the new material is convenient for installation of a MCFC stack due to its good strength and its ability to convert in situ into the working cathodes during the MCFC startup stage. Also, the very short preparation time for the new material is suitable for industrial production on a large scale.

References:

[1] Mitsushima S, Matsuzawa K, Kamiya N, et al. *Electrochim. Acta*, **2002**,**47**:3823-3830

[2] Wee J H, Lee K Y. *J. Mater. Sci.*, **2006**,**41**:3585-3592

[3] Plomp L, Sitters E F, Vessies C, et al. *J. Electrochem. Soc.*, **1991**,**138**:629-630

[4] Plomp L, Veldhuis J B J, Sitters E F, et al. *J. Power Sources*, **1992**,**39**:369-373

[5] Giorgi L, Carewska M, Scaccia S, et al. *J. Hydrogen Energy*, **1996**,**21**:491-496

[6] Fukui T, Okawa H, Tsunooka T. *J. Power Sources*, **1998**,**71**: 239-243

[7] Lundblad A, Schwartz S, Bergman B. *J. Power Sources*, **2000**, **90**:224-230

[8] Kim S G, Yoon S P, Han J, et al. *J. Power Sources*, **2002**,**112**: 109-115

[9] Wijayasinghe A, Lagergren C, Bergman B. *Fuel Cells*, **2002**,**2**: 181-187

[10]Wijayasinghe A, Bergman B, Lagergren C. *Solid State Ionics*, **2006**,**177**:165-173

[11]Wijayasinghe A, Bergman B, Lagergren C. *Solid State Ionics*, **2006**,**177**:175-184

[12]Ringuede A, Wijayasinghe A, Albin V, et al. *J. Power Sources*, **2006**,**160**:789-795

[13]Milanese C, Berbenni V, Bruni G, et al. *Solid State Ionics*, **2006**,**177**:1893-1896

[14]Kuk S T, Song Y S, Kim K. *J. Power Sources*, **1999**,**83**:50-56

[15]Chen L J, Zuo J, Lin C J. *Fuel Cells*, **2003**,**3**:220-223

[16]Kim S G, Yoon S P, Han J, et al. *Electrochim. Acta*, **2004**,**49**: 3081-3089

[17]Fukui T, Okawa H, Hotta T, et al. *J. Am. Ceram. Soc.*, **2001**, **84**:233-235

[18]Fukui T, Ohara S, Okawa H, et al. *J. Power Sources*, **2000**,**86**: 340-346

[19]Lee H S, Hong M Z, Park E J, et al. *J. Mater. Sci.*, **2004**,**39**: 5595-5598

[20]Lee H, Hong M Z, Bae S C, et al. *J. Mater. Chem.*, **2003**,**13**: 2626-2632

[21]Kim Y S, Yi C W, Choi H S, et al. *J. Power Sources*, **2011**, **196**:1886-1893

[22]Kim M H, Hong M Z, Kim Y S, et al. *Electrochim. Acta*, **2006**,**51**:6145-6151

[23]Daza L, Rangel C M, Baranda J, et al. *J. Power Sources*, **2000**,**86**:329-333

[24]Soler J, Gonzalez T, Escuderoa M J, et al. *J. Power Sources*, **2002**,**106**:189-195

[25]Huang B, Yu Q C, Wang H M, et al. *J. Power Sources*, **2004**, **137**:163-174

[26]Kuk S T, Song Y S, Suh S, et al. *J. Mater. Chem.*, **2001**,**11**: 630-635

[27]Hong M Z, Bae S C, Lee H S, et al. *Electrochim. Acta*, **2003**, **48**:4213-4221

[28]Chen L J, Lin C J, Cheng X, et al. *Solid State Ionics*, **2002**, **148**:539-544

[29]Chen L J, Lin C J, Huang C M. *Electrochim. Acta*, **2002**,**47**: 3515-3522